

Transcriptional Regulation of Bim by FoxO3A Mediates Hepatocyte Lipoapoptosis*

Received for publication, May 29, 2007, and in revised form, July 5, 2007. Published, JBC Papers in Press, July 11, 2007, DOI 10.1074/jbc.M704391200

Fernando J. Barreiro, Shogo Kobayashi, Steven F. Bronk, Nathan W. Werneburg, Harmeet Malhi, and Gregory J. Gores¹

From the Division of Gastroenterology and Hepatology, Mayo Clinic College of Medicine, Rochester, Minnesota 55905

Hepatocyte lipoapoptosis, a critical feature of nonalcoholic steatohepatitis, can be replicated *in vitro* by incubating hepatocytes with saturated free fatty acids (FFA). These toxic FFA induce Bim expression, which is requisite for their cytotoxicity. Because the FoxO3a transcription factor has been implicated in Bim expression, our aim was to determine if FFA induce Bim by a FoxO3a-dependent mechanism. In Huh-7 cells, the saturated FFA, palmitic and stearic acid, increased Bim mRNA 16-fold. Treatment of cells with the saturated FFA induced FoxO3a dephosphorylation (activation) and nuclear translocation and stimulated a FoxO luciferase-based reporter assay; direct binding of FoxO3a to the Bim promoter was also confirmed by a chromatin immunoprecipitation assay. A small interfering RNA-targeted knockdown of FoxO3a abrogated FFA-mediated Bim induction and apoptosis. FoxO3a was activated by a phosphatase 2A-dependent mechanism, since okadaic acid- and small interfering RNA-targeted knockdown of this phosphatase blocked FoxO3a dephosphorylation, Bim expression, and apoptosis. Consistent with these data, phosphatase 2A activity was also stimulated 3-fold by saturated FFA. Immunoprecipitation studies revealed an FFA-dependent association between FoxO3a and protein phosphatase 2A. FFA-mediated FoxO3a activation by protein phosphatase 2A was also observed in HepG2 cells and murine hepatocytes. In conclusion, saturated FFA stimulate protein phosphatase 2A activity, which activates FoxO3a, inducing expression of the intracellular death mediator Bim.

Nonalcoholic fatty liver disease is present in up to 30% of the American population (1). A subset of these individuals, ~5%, develop hepatic inflammation, a syndrome referred to as non-alcoholic steatohepatitis (NASH)² (2). This hepatic inflammatory disorder can progress to cirrhosis, chronic liver disease with portal hypertension, and hepatocellular carcinoma (2). A

major risk factor for NASH is insulin resistance occurring within the context of the metabolic syndrome (3, 4). Insulin resistance results in excessive lipolysis within peripheral adipose tissue (5). This lipolysis liberates free fatty acids from neutral fat. The liberated intracellular free fatty acids (FFA) are released into the serum, where they are taken up by the liver (6). Indeed, the bulk of hepatic neutral fat in NASH is derived from re-esterification of circulating FFA (6). Given this information, it is not surprising that elevated serum FFA are a hallmark of NASH (7, 8), and the magnitude of circulating FFA correlates with liver disease severity (7). Therapies that improve NASH by enhancing insulin sensitivity also decrease plasma FFA (9). Thus, FFA probably play an integral role in the development and progression of NASH.

FFA appear to cause liver injury by inducing hepatocyte apoptosis, a phenomenon termed lipoapoptosis (10, 11). Indeed, hepatocyte apoptosis is a cardinal feature of NASH and correlates with hepatic inflammation and fibrosis (8, 12). Consistent with this concept, elevated serum cytokeratin-18 fragments, markers of hepatocyte apoptosis, distinguish simple hepatic steatosis from NASH (13). FFA also induce hepatocyte apoptosis *in vitro*; in this model, saturated FFA (*e.g.* stearic or palmitic acid) are more toxic than the unsaturated FFA (*e.g.* oleic acid). Toxic, saturated FFA induce hepatocyte apoptosis, in part, by the up-regulation of Bim (Bcl-2-interacting mediator of cell death), a proapoptotic member of the Bcl-2 (B-cell lymphoma 2) protein family (10). In fact, FFA-mediated hepatocyte apoptosis is abrogated by siRNA-targeted knockdown of Bim (10). Bim belongs to a subset of the Bcl-2 protein family which displays sequence conservation exclusively in the short Bcl-2 homology 3 (BH3) domain and are referred to as BH3-only proteins. These proteins are biosensors of cellular stress and induce apoptosis by functioning as intracellular death ligands (14). BH3-only proteins such as Bim bind to multidomain members of the Bcl-2 family, causing mitochondria dysfunction, with release of proapoptotic factors into the cytosol (*e.g.* cytochrome *c*, SMAC/Diablo, endonuclease G, and AIF) (15). Cytosolic cytochrome *c* promotes activation of downstream effector caspase-3 and -7, proteases that dismantle the cell, causing cell death by apoptosis (16). Bim exists at the protein level as three isoforms, including Bim extra long (BimEL), Bim long (BimL), and Bim short (BimS) (17). All three isoforms are regulated by both transcriptional and post-transcriptional mechanisms. FFA markedly enhance cellular Bim mRNA levels and therefore probably regulate Bim expression by a transcriptional mechanism (10).

* The costs of publication of this article were defrayed in part by the payment of page charges. This article must therefore be hereby marked "advertisement" in accordance with 18 U.S.C. Section 1734 solely to indicate this fact.

¹ To whom correspondence should be addressed: Mayo Clinic College of Medicine, 200 First St. SW, Rochester, MN 55905. Tel.: 507-284-0686; Fax: 507-284-0762; E-mail: gores.gregory@mayo.edu.

² The abbreviations used are: NASH, nonalcoholic steatohepatitis; BH3, Bcl-2 homology domain 3; DAPI, 4',6'-diamidino-2-phenylindole; FFA, free fatty acid(s); JNK, c-Jun N-terminal kinase; PP1, protein phosphatase type 1; PP2A, protein phosphatase type 2A; PBS, phosphate-buffered saline; siRNA, small interfering RNA; SGK, serum- and glucocorticoid-induced kinase; HA, hemagglutinin; Ab, antibody; PA, palmitic acid; SA, stearic acid; OA, oleic acid; Veh, vehicle.

Bim mRNA expression is regulated by a member of the FoxO (Forkhead box-containing protein, class O) family of transcription factors, FoxO3a (18–20). This transcription factor is deactivated by kinase-directed phosphorylation and activated by phosphatase-mediated dephosphorylation (21, 22). FoxO3a factor resides in the nucleus, where it is a positive regulator of gene expression. However, upon phosphorylation, FoxO3a is transported out of the nucleus and sequestered in the cytosol, where it is bound to the protein 14-3-3 (21). Once sequestered in the cytoplasm, it can be reactivated by dephosphorylation via a serine/threonine phosphatase pathway (22).

Both Akt and serum- and glucocorticoid-induced kinase (SGK) phosphorylate FoxO3a at the same sites, albeit with different affinities, Thr³², Ser²⁵³, and Ser³¹⁵ (23, 24). There is cooperativity between these sites such that identification of Thr³² phosphorylation can be used to indicate phosphorylation of the other two sites (24). Reactivation of phosphorylated FoxO3a probably occurs via the ubiquitous threonine/serine phosphatase, protein phosphatase 2A (22). Thus, both cellular localization, nuclear *versus* cytosolic, and Thr³² phosphorylation (negative regulator) can be used to assess the FoxO3a activation status.

The major objectives of this study were to determine if FFA regulate Bim expression via FoxO3a. The results indicate that toxic FFA preferentially induce Bim expression and cell death by a FoxO3a-dependent mechanism. This activation (dephosphorylation) of FoxO3a is mediated by FFA-stimulated protein phosphatase 2A activity.

EXPERIMENTAL PROCEDURES

Cells—Huh-7 cells, a human hepatoma cell line, and HepG2 cells, a human hepatoblastoma cell line, were cultured in Dulbecco's modified Eagle's medium containing high glucose (25 mM), 100,000 units/liter penicillin, 100 mg/liter streptomycin, and 10% fetal bovine serum. Mouse hepatocytes were isolated from C57BL/6 (Jackson Laboratories, Bar Harbor, ME) by collagenase perfusion, purified by Percoll gradient centrifugation, and plated as primary cultures (25).

Plasmid and Transfection—The HA-FoxO3a expression plasmid was kindly provided by M. C. Hung (26). Transfection with HA-FoxO3a was performed using Lipofectamine (Invitrogen). Stably transfected clones were selected in medium containing 1200 mg/liter G418 and screened by immunoblot analysis.

Fatty Acid Treatment—Stearic, palmitic, and oleic acid were from Sigma. All three FFA were individually dissolved in isopropyl alcohol at a concentration of 40 mM. Dulbecco's modified Eagle's medium containing 1% bovine serum albumin was used in all experiments. The concentration of fatty acids used was 400 μ M. The concentration of the vehicle, isopropyl alcohol, was 1% in final incubations. Control cells were treated with vehicle alone. Cells were treated when ~60% confluent.

Quantitation of Apoptosis—Nuclei were stained with 5 μ g/ml 4',6-diamidino-2'-phenylindole dihydrochloride (DAPI) for 30 min at room temperature and visualized under fluorescence microscopy (Nikon Eclipse TE200, Nikon Corporation, Japan). Apoptotic cells were quantified by counting 400 random cells per study. Cells with the characteristic nuclear

changes of chromatin condensation and nuclear fragmentation were considered apoptotic. Apoptosis was expressed as a percentage of total cells counted.

Caspase-3/7 Activity—Cells were plated in 96-well plates (Corning Glass). A caspase assay was performed using the commercially available Apo-ONE homogeneous caspase-3/7 assay (Promega Corp.) according to the manufacturer's instructions. Briefly, this assay involves cleavage of a profluorescent caspase-3/7 consensus substrate, bis-(*N*-benzyloxycarbonyl-L-aspartyl-L-glutamyl-L-valyl-aspartic acid amide) conjugated to rhodamine 110 (benzyloxycarbonyl-DEVD-R110) on its C-terminal side. Proteolytic cleavage liberates rhodamine 110, unquenching its fluorescence, and was measured using excitation and emission wavelengths of 498 and 521 nm, respectively. Fluorescence intensity was acquired by a microplate fluorescence reader (FLx800; Bio-Tek Instruments Inc., Winooski, VT). The amount of fluorescent product generated is proportional to the amount of caspase-3/7 cleavage activity present in the sample.

Immunocytochemistry—Cells were cultured on collagen-coated coverslips. The medium was aspirated, and the cells were washed three times with PBS and then fixed with freshly prepared 4% paraformaldehyde for 20 min at room temperature. After another washing step with PBS, cells were permeabilized using 0.2% Triton X-100 in PBS for 20 min at room temperature. Next the cells were incubated in PBS containing 10% fetal bovine serum, 0.1 N Na₃N₃, and 0.1% Triton X-100 at room temperature for 20 min. Primary antibody incubation was carried out with anti-FoxO3a (1:200 dilution, rabbit, 07-702; Upstate Biotechnology, Inc., Lake Placid, NY) for 1 h at room temperature. After another washing step with PBS, the cells were incubated with the secondary antibody, Cy3-conjugated anti-rabbit antibody (1:1000; Jackson Immunological Research Laboratories, Inc.), for 30 min at room temperature. All antibodies were diluted in PBS plus 5% fetal bovine serum. The slides were stained with 0.2 μ g/ml DAPI diluted in PBS for 5 min at room temperature and then washed three times in PBS. Next, the coverslips were removed, and Prolong antifade (Molecular Probes, Inc., Eugene, OR) was used as mounting medium. Images were acquired by confocal microscopy with an inverted Zeiss laser-scanning confocal microscope (Zeiss LSM 510; Carl Zeiss Inc., Thornwood, NJ). Individual nuclei were outlined using DAPI fluorescence, and the nuclear fluorescence of Cy3 was quantified using Zeiss KS400 image analysis software (Carl Zeiss, Inc., Oberkochen, Germany). Nuclear FoxO3a fluorescence was expressed as an increase in total nuclear fluorescence intensity per cell (pixels above threshold \times fluorescence intensity).

Immunoblot Analysis—Cells were lysed for 30 min on ice with lysis buffer (50 mM/liter Tris-HCl (pH 7.4), 1% Nonidet P-40, 0.25% sodium deoxycholate, 150 mM NaCl, 1 mM EDTA, 1 mM phenylmethylsulfonyl fluoride, 1 μ g/mol aprotinin, 1 μ g/mol leupeptin, 1 μ g/mol pepstatin, 1 M Na₃VO₄, and 1 mM NaF). After centrifugation at 13,000 \times g for 15 min, protein concentration in the supernatant was measured using Bradford's reagent (Bio-Rad). The supernatant protein was denatured by boiling for 10 min. Protein (40 μ g) was resolved by SDS-PAGE on a 4–15% gradient gel and then transferred onto nitrocellulose membranes. Blocking was carried out using 5%

nonfat dry milk in Tris-buffered saline (20 mM Tris, 150 mM NaCl, pH 7.4) with 0.1% Tween 20 for 2 h at room temperature. Primary antibodies (Ab) were diluted in blocking solution and incubated overnight at 4 °C: polyclonal Ab to FoxO3a (7-702) and polyclonal Ab to phospho-FoxO3a (Thr³²) (7-695) (rabbit, 1:1000 dilution; Upstate Biotechnology); monoclonal Ab to Bim (MAB17001) (rat, 1:1000 dilution; Chemicon, Australia); monoclonal Ab to phospho-Akt (Ser⁴⁷³) (4051) (mouse, 1:1000 dilution; Cell Signaling Technology, Danvers, MA); polyclonal Ab to Akt (9272) (rabbit, 1:1000 dilution; Cell Signaling Technology); polyclonal Ab to IKK- β (2684) (rabbit, 1:1000 dilution; Cell Signaling Technology); polyclonal Ab to phospho-IKK- α/β (2694) (rabbit, 1:1000 dilution; Cell Signaling Technology); polyclonal Ab to I κ B- α (sc-371) (goat, 1:500 dilution; Santa Cruz Biotechnology, Inc., Santa Cruz, CA); polyclonal Ab to PP2A catalytic subunit α isoform clone 1D6 (05-421) (mouse, 1:5000 dilution; Upstate Biotechnology); monoclonal phospho-PP2A (Tyr³⁰⁷) (1155-1) (rabbit, 1:5000 dilution; Epitomics, Burlingame, CA); polyclonal Ab to PTEN (9552) (rabbit, 1:1000 dilution; Cell Signaling Technology); polyclonal Ab to phospho-PTEN (Ser³⁸⁰/Thr^{382/383}) (9554) (rabbit, 1:1000 dilution; Cell Signaling Technology, Danvers, MA); polyclonal Ab to SGK (3272) (rabbit, 1:1000 dilution; Cell Signaling Technology, Danvers, MA); polyclonal Ab to phospho-SGK (Ser²⁵⁵/Thr²⁵⁶) (9554) (rabbit, 1:1000 dilution; Upstate Technology); monoclonal Ab to γ -tubulin (T6557) (mouse, 1:5000 dilution; Sigma); polyclonal Ab to actin (sc-1615) (goat, 1:2000 dilution; Santa Cruz Biotechnology). To detect antigen-antibody complexes, peroxidase-conjugated secondary antibodies (1:3000; BIOSOURCE, Camarillo, CA) were diluted in blocking solution and incubated for 45 min at room temperature. Immune complexes were visualized using a chemiluminescent substrate (ECL; Amersham Biosciences), and Eastman Kodak Co. X-Omat film.

Immunoprecipitation—Immunoprecipitation for HA-FoxO3a was performed with 2 μ g of anti-HA (rat monoclonal Ab; Roche Applied Science) or 2 μ g of anti-PP2A-C (Upstate Biotechnology) in 1.0 mg of whole lysate protein. Samples were first precleared with protein G-Sepharose (Zymed Laboratories, Inc.) for 30 min. Precleared lysates were centrifuged to discard the beads and incubated with anti-HA or anti-PP2A-C for 4 h and then incubated overnight with protein G-Sepharose. Samples were washed six times with lysis buffer and then subjected to immunoblot analysis as described above.

Akt and Phospho-Akt Immunoreactivity by Enzyme-linked Immunosorbent Assay—Akt and phospho-Akt immunoreactivity were measured using a commercially available fast activated cell-based enzyme-linked immunosorbent assay (Active Motif, Carlsbad, CA). Briefly, cells were plated in 96-well plates. Cells were fixed with 4% formaldehyde followed by quenching of endogenous peroxidase with 1% H₂O₂ and 0.1% sodium azide in PBS containing 0.1% Triton X-100. Each well was incubated with antibody specific to total Akt or phospho-Akt. Horseradish peroxidase-conjugated secondary antibody was subsequently added and developed with the commercial reagent. Absorption was measured at 450 nm using a spectrophotometer. Cell number was quantitated by crystal violet staining. Akt and phospho-Akt immunoreactivity was normalized to cell number.

Reporter Gene Assay—The luciferase reporter construct 3 \times IRS-Luc, which contains three copies of the FoxO-responsive element from the IGFBP1 promoter, was obtained from K. L. Guan (27). Twenty-four hours after the transfection, cells were incubated with 400 μ M FFA, and control cells were incubated with vehicle alone for 6 h. Cells were washed two times with PBS, and then cell lysates were prepared by adding lysis buffer directly to the cells for 20 min at 4 °C on a rocking shaker platform. Next, both firefly and *Renilla* luciferase activities were quantitated using the dual luciferase reporter assay system (Promega, Madison, WI) according to the manufacturer's instructions. Luciferase was quantified using a luminometer (TD-20/20, Turner Designs, Sunnyvale, CA).

Real Time Polymerase Chain Reaction—Total RNA was extracted from the cells using the Trizol reagent (Invitrogen) and was reverse-transcribed into complementary DNA with Moloney leukemia virus reverse transcriptase and random primers (both from Invitrogen). Quantification of the complementary DNA template was performed with real time PCR (LightCycler; Roche Applied Science) using SYBR green (Molecular Probes) as a fluorophore. PCR primers were as follows: for human *BIM*, forward (5'-TATGAGAAGATCCTCCCTGC-3') and reverse (5'-ATATCTGCAGGTTTCAGCCTG-3'); for human *PP2A-C α* , forward (5'-GAATCCAACGTGCAAGAGGT-3') and reverse (5'-CGTTCACGGTAACGAACCTT-3'); for human *PP1C*, forward (5'-GACAGCGAGAAGCTCAACCT-3') and reverse (5'-CTCCAGCTCCAGAAGAA-TGG-3'); for murine *bim*, forward (5'-CGACAGTCTCAGGAGGAACC-3') and reverse (5'-CCTTCTCCATACCAGACGGA-3'). As an internal control, primers for 18 S ribosomal RNA were purchased from Ambion (Austin, TX). After electrophoresis in 2% agarose gel, each expected base pair PCR product was cut out and eluted into Tris-HCl using a DNA elution kit (gel extraction kit; Qiagen, Valencia, CA). The concentrations of extracted PCR products (copies/ μ l) were measured using a spectrophotometer at 260 nm and were used to generate standard curves. The inverse linear relationship between copy and cycle numbers was then determined. Each resulting standard curve was then used to calculate the number of copies/ μ l in experimental samples. The relative expression level of each product was expressed as a ratio of 18 S ribosomal copies of PCR product for each sample.

siRNA-targeted Knockdown of FoxO3a and PP2A—RNA interference was used to knock down FoxO3a and PP2A protein expression in Huh-7 cells. The FoxO3a siRNA sequence corresponds to the coding region 46–64 relative to the first nucleotide of the start codon. FoxO3a sense (5'-ACUC-CGGGUCCAGCUCCAC(dTdT)-3')/FoxO3a antisense (5'-GUGGAGCUGGACCCGGAGU(dTdT)-3') targeting human FoxO3a was synthesized using the Silencer siRNA construction kit (Ambion). The protein phosphatase 2A, catalytic subunit, α isoform (siRNA-PP2A-C) was purchased from Dharmacon (Lafayette, CO). As a control, cells were also transfected with scrambled RNA duplex with the sequence 5'-AACGTGATT-TATGTCACCAGA-3'. FoxO3a and PP2A-C knockdown were performed by transfection of siRNA into cells using siPORT lipid transfection reagent according to the manufacturer's instructions. Successful targeted knockdown was verified by

real time PCR after transient transfection of the cells with siRNA. Briefly, cells were grown in 12-well dishes and were transiently transfected with 50 nM siRNA-FoxO3a or 100 nM siRNA-PP2A-C, using 6 μ l/ml siPORT lipid (Ambion) in a total transfection volume of 0.5 ml of Opti-MEM (Invitrogen). After incubation at 37 °C, 5% CO₂ for 4 h, 1 ml of normal growth medium was added. Transfected cells were then analyzed for apoptosis, immunoblot, and real time PCR as described elsewhere under "Experimental Procedures."

Chromatin Immunoprecipitation Assay—Chromatin immunoprecipitation assay was performed using a commercially available assay kit (Upstate Biotechnology) according to the manufacturer's instructions. Briefly, cells were incubated with 1% formaldehyde in media at 37 °C for 20 min to cross-link DNA and DNA-binding proteins. After washing in PBS, cells were collected and lysed within 200 μ l of SDS lysis buffer supplied by the kit. DNA within the cell extracts was sheared by sonication with four sets of 10-s pulses using a sonicator (Soni-fier cell disruptor; Heat Systems-Ultrasonics, Plainview, NY) equipped with a 2-mm tip and set to 30% of maximum power. The cell lysates were next subjected to 13,000 $\times g$ for 10 min. The DNA concentration in the supernatant was quantified by measuring absorbance at 260 nm. Samples containing 200 μ g of DNA were diluted with the chromatin immunoprecipitation dilution buffer to a final volume of 2,050 μ l. Fifty microliters from each sample were removed as a nonimmunoprecipitation input control. After preclearing the sample with 75 μ l of salmon sperm DNA/protein A-agarose slurry at 4 °C for 30 min, the target protein FoxO3a was immunoprecipitated with 2 μ g of anti-FoxO3a polyclonal antibody (Upstate Biotechnology) at 4 °C overnight with rotation using a multipurpose rotator (model 151; Scientific Industries, Bohemia, NY). A mock immunoprecipitation without antibody was also performed. Next, 60 μ l of the salmon sperm DNA/protein A-agarose slurry was added and incubated at 4 °C for 60 min. After washing the agarose beads, the protein A-agarose immune complexes were eluted, in two separate 250- μ l aliquots, in elution buffer (1% SDS, 0.1 mol/liter NaHCO₃) at room temperature for 30 min. Twenty-five microliters of each eluent was used for immunoblot analysis to determine the immunoprecipitation efficiency. Following the addition of 5 M NaCl (20 μ l), protein-DNA cross-linking was reversed by heating at 65 °C for 6 h. After digestion with 2 μ l of 10 mg/ml proteinase K at 45 °C for 1 h, DNA fragments were purified via phenol/chloroform extraction and ethanol precipitation, and the DNA pellet was dissolved in 20 μ l of water. The following PCR primers were employed to amplify the product spanning the FoxO3a-specific binding site identified in the 5'-flanking region of the human *BIM* gene: forward, 5'-TCGCGAGGACCAACCCAGTC-3'; reverse, 5'-CCGCTCCTACGCCCAATCAC-3'. The copy number for amplified PCR products was quantitated using real time PCR.

Protein Phosphatase 2A Activity—A commercially available PP2A immunoprecipitation phosphatase assay kit (Upstate Biotechnology) was used to measure phosphate release as an index of phosphatase activity. Briefly, Huh-7 cells and HepG2 cells were treated with 400 μ M FFA for 6–8 h, and vehicle was used as control. Then total cellular proteins were extracted in a phosphatase extraction buffer (100 mM Tris-HCl, pH 7.6, 100

mM NaCl, 2 mM MgCl₂, 1 mM CaCl₂, 2 mM EGTA, 1% Triton X-100, 1 mM phenylmethylsulfonyl fluoride, and the protease inhibitor tablet c-complete (Roche Applied Science)), sonicated for 10 s, and spun down. To preclear protein extracts, protein A-agarose slurry was added, followed by rotation at 4 °C for 1 h. Samples were centrifuged to discard the beads, and 1000 μ g of total cellular protein was incubated with protein A-agarose slurry with anti-PP2A-C (2 μ g/ml, catalog number 05-421; Upstate Biotechnology) or anti-PP1-catalytic subunit (PP1C) (2 μ g/ml, sc-7482; Santa Cruz Biotechnology) at 4 °C with constant rocking for overnight. Agarose-bound immune complexes were collected and, following washing with 500 μ l of Tris-buffered saline (five times) and 500 μ l of optimized Ser/Thr buffer (final wash), were resuspended in 50 μ l of Ser/Thr buffer. Then 25 μ l/sample were incubated with 250 μ M of phosphopeptide (amino acid sequence KRpTIRR (where pT represents phosphothreonine), obtained from the kit) or 250 μ M phospho-FoxO3a peptide (amino acid sequence SCpTWPL, FoxO3a amino acids 30–35, synthesized by the Mayo Clinic Proteomics Core), in a total volume of 50 μ l. The reaction was started by the addition of the phosphopeptide or phospho-FoxO3a peptide and conducted for 10 min at room temperature in a shaking incubator. Supernatants (25 μ l) were transferred in a 96-well plate, and released phosphate was measured by adding 100 μ l of malachite green phosphate detection solution. Color was developed for 10 min before reading the plate at 650 nm. The absorbance of the reactions was corrected by subtracting the absorbance in samples treated without Ab. Phosphate concentrations were calculated from a standard curve created using serial dilutions of a standard phosphate solution (0–2,000 pmol). Results were expressed as -fold change of PP2A activity as compared with that of vehicle-treated cells.

Reagents—DAPI, stearic acid (S4751), palmitic acid (P0500), oleic acid (O1008), fumonisins B1 (F1147), 1,2-dioleoyl-*sn*-glycero-3-phosphate (42491), and actinomycin D (A9415) were from Sigma. Okadaic acid (E1181) was from Biomol Research Laboratories (Plymouth Meeting, PA). The phosphatidylinositol 3-kinase inhibitor LY294002 (440202) and the JNK inhibitor SP600125 (420119) were from Calbiochem.

Statistical Analysis—All data represent at least three independent experiments and are expressed as the means \pm S.E. of the mean. Differences between groups were compared using Student's *t* tests and one-way analysis of variance with *post hoc* Dunnett test, and significance was accepted at *p* < 0.05.

RESULTS

The Saturated FFA, Palmitic and Stearic Acid, Preferentially Induce *Bim* Expression—Given that our prior studies were predominantly in HepG2 cells (10), we first established that FFA induce *Bim* expression in Huh-7 cells by real time PCR and immunoblot analysis (Fig. 1). The saturated FFA, stearic and palmitic acid, at a concentration of 400 μ M increased *Bim* mRNA between 15- and 20-fold after 8 h of incubation (Fig. 1A). In contrast, under identical conditions, the monounsaturated FFA, oleic acid, only increased *Bim* mRNA expression 3-fold. In the Huh-7 cells, only *Bim*_{EL} was readily identified by immunoblot analysis (Fig. 1B). Consistent with the real time PCR data, both stearic and palmitic acid increased cellular

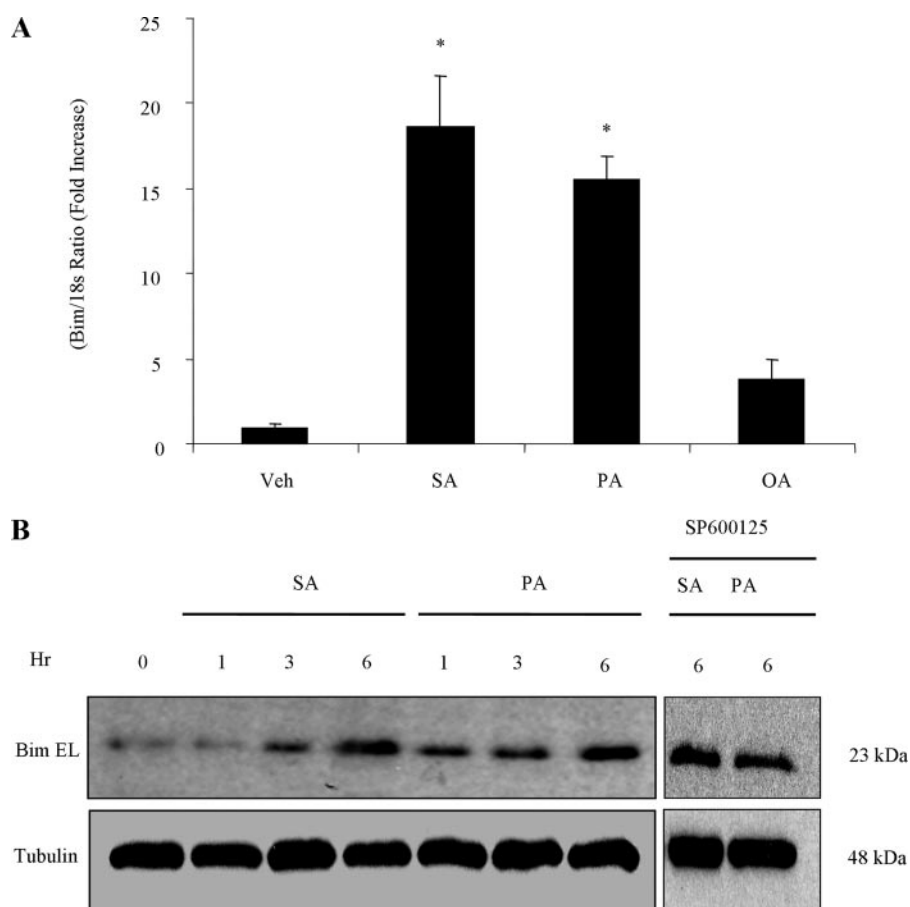


FIGURE 1. Saturated FFA increase Bim expression. *A*, Huh-7 cells were treated with palmitic acid (PA), stearic acid (SA), and oleic acid (OA) at 400 μ M for 8 h, and vehicle (Veh) was used as control. Bim mRNA was quantified by real time PCR. -Fold induction was determined after normalization to 18 S. Data represent the mean and error of five independent experiments. *, $p < 0.05$. *B*, whole cell lysates were analyzed for Bim protein expression at the time points indicated following treatment with FFA. The JNK inhibitor SP600125 (10 μ M) was used in the presence of SA and PA at 400 μ M for 6 h (Hr). Tubulin was used as control for protein loading.

Bim_{EL} protein expression (Fig. 1*B*), whereas oleic acid had only a minimal effect on cellular Bim_{EL} protein levels (data not shown). These data in Huh-7 cells confirm our prior observations in HepG2 cells that saturated FFA increase Bim mRNA and protein expression. This paradigm, enhanced Bim expression by saturated FFA, provided us with a model to dissect the signaling pathways responsible for this observation. We selected Huh-7 cells in this model, because they can be transfected with greater efficiency than HepG2 cells. Finally, although we have previously demonstrated that the JNK inhibitor SP600125 reduces FFA-mediated Bax (Bcl-2-associated x protein) activation, it does not prevent Bim protein induction (Fig. 1*B*); nor does it reduce Bim mRNA (data not shown). Based on this information, we focused our current studies on FoxO3a regulation of Bim expression.

Saturated FFA Dephosphorylate and Activate FoxO3a—Under basal conditions, FoxO3a was phosphorylated at Thr³² as assessed by phosphoimmunoblot analysis; however, FoxO3a was dephosphorylated (activated) after incubation of Huh-7 cells with stearic or palmitic acid (Fig. 2, *A* and *B*). FoxO3a dephosphoryla-

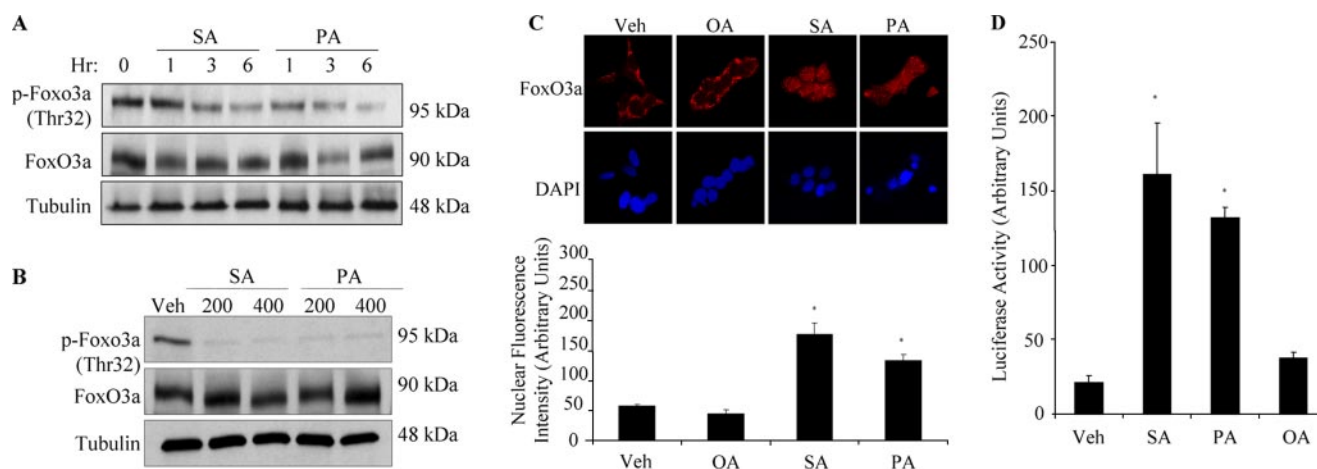


FIGURE 2. Saturated FFA activate FoxO3a. *A*, Huh-7 cells were treated with 400 μ M SA or PA, respectively, for the indicated time intervals. Whole cell lysates were analyzed for protein expression using antibodies specific to total and phosphorylated (inactive form) FoxO3a. Tubulin was used as control for protein loading. *B*, Huh-7 cells were treated with SA or PA (200 and 400 μ M, respectively) for 6 h. Total and phospho-FoxO3a protein levels were assessed by immunoblot analysis. Tubulin was used as control for protein loading. *C*, Huh-7 cells were examined by immunofluorescence microscopy after treatment with OA, SA, and PA (400 μ M) for 4 h; Veh-treated cells were used as controls. Huh-7-treated cells were fixed and stained with DAPI to visualize nuclei, and FoxO3a cellular localization was detected by immunofluorescence. Representative images from three independent experiments are depicted. Fluorescent images were acquired by confocal microscopy. Nuclear FoxO3a fluorescence was expressed as an increase in total nuclear fluorescence intensity per cell (pixels above threshold \times fluorescence intensity). Data represent mean \pm S.E. of three experiments. *D*, Huh-7 cells were transfected with a FoxO luciferase reporter gene construct. At 24 h after transfection, the cells were incubated with SA, PA, or OA (400 μ M) for an additional 8 h. Results are expressed as -fold change from vehicle-treated cells. Data represent mean \pm S.E. of five separate experiments. *, $p < 0.05$.

tion by palmitic acid and stearic acid was time-dependent and observed at concentrations of either 200 or 400 μM . Oleic acid treatment resulted in less FoxO3a dephosphorylation as compared with the saturated FFA (data not shown). More importantly, as assessed by immunocytochemistry, palmitic and stearic acid, but not oleic acid, promoted the translocation of FoxO3a from the cytoplasm to the nucleus (Fig. 2C). To determine whether the nuclear FoxO3a was transcriptionally active, Huh-7 cells were transfected with a luciferase reporter construct containing three copies of a FoxO response element. Following incubation with 400 μM stearic and palmitic acid for 8 h, luciferase activity increased over 6-fold (Fig. 2D). Taken together, these results demonstrate activation of the transcription factor FoxO3a by the toxic, saturated FFA, stearic and palmitic acid.

Bim Induction by FFA Is FoxO3a-dependent—Having demonstrated that toxic, saturated FFA can activate FoxO3a, we next determined if their induction of Bim is FoxO3a-dependent. A chromatin immunoprecipitation assay was performed to confirm that FoxO3a binds to a putative cognate binding sequence within the *bim* promoter (Fig. 3A). The amount of precipitated FoxO3a-Bim promoter complex was significantly increased after treatment with either stearic or palmitic acid (Fig. 3A). Although these data demonstrate that FoxO3a binds to the Bim promoter in response to FFA exposure and support an effect on Bim gene transcription, they do not exclude an effect of FFA on Bim mRNA half-life. To more directly address this potential mechanism of Bim regulation, the effect of the saturated FFA (palmitic acid) on Bim mRNA half-life was assessed by quantifying Bim mRNA over time in FFA-treated cells incubated in the presence of actinomycin D, a transcription inhibitor. FFA treatment, however, did not increase the half-life of Bim mRNA (Fig. 3B). To more rigorously ascertain whether other potential pathways and transcription factors could account for induction of Bim by FFA, an siRNA approach was undertaken to knock down FoxO3a. The siRNA targeting FoxO3a employed for these studies markedly reduced FoxO3a cellular protein levels (Fig. 4A) and completely abrogated induction of Bim mRNA and protein by stearic and palmitic acid (Fig. 4, A and B). The siRNA knockdown of FoxO3a was specific, since it had no effect on FoxO1 cellular protein levels (Fig. 4A). Accordingly, FoxO3a knockdown also conferred protection against FFA-mediated apoptosis as assessed both by morphology and caspase-3/7 activity (Fig. 5, A and B). These results appeared to be specific for FoxO3a, since FoxO1 protein levels were unchanged using siRNA to FoxO3a (Fig. 4A). Collectively, these data implicate FoxO3a as a key regulator of Bim expression during FFA-mediated lipotoxicity.

FFA Activation of FoxO3a Requires Protein Phosphatase Activity—The phosphorylation status of a protein represents a balance between direct kinase phosphorylation and phosphatase dephosphorylation. Therefore, we explored this balance in FFA-mediated FoxO3a dephosphorylation. Because FoxO3a is phosphorylated and, therefore, inactivated by the serine/threonine kinases phospho-AKT and phospho-SGK (active forms) (24), we first postulated that saturated FFA would inhibit pathways leading to Akt and SGK activation. Unexpectedly, FFA did not significantly alter cellular levels of active phospho-AKT and

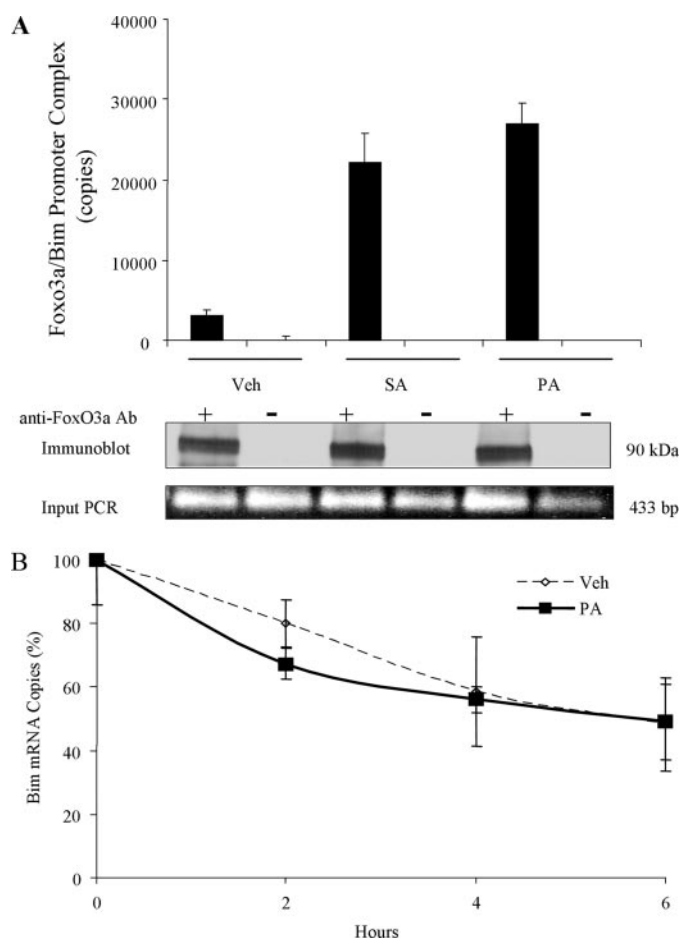


FIGURE 3. Saturated FFA increase FoxO3a binding to the Bim promoter and regulate Bim mRNA expression. A, Huh-7 cells were treated with SA, PA, and OA (400 μM) for 6 h. Veh was used as a control. Next, the cells were fixed and lysed, and immunoprecipitation for FoxO3a was performed. Then PCR for the FoxO3a consensus binding site within the *bim* promoter was performed using the DNA. Data were expressed as copies of the FoxO3a promoter from three independent experiments. Data are mean \pm S.E. *, $p < 0.05$. B, Huh-7 cells were treated with PA (400 μM) or vehicle at the indicated time intervals, in the presence of 2 $\mu\text{g}/\text{ml}$ actinomycin D. At each indicated time point, total cellular RNA was extracted and analyzed by real time PCR as described under "Experimental Procedures." Results are expressed as a percentage change of Bim mRNA copies as compared with time 0. Data represent mean \pm S.E. from three independent experiments.

phospho-SGK by phosphoimmunoblot analysis (Fig. 6) and enzyme-linked immunosorbent assay (data not shown). In particular, FFA treatment did not reduce the active (phospho) levels of these kinases, which would be necessary for FoxO3a activation. Given these results, we next examined the role of phosphatase activity in FFA-mediated FoxO3a dephosphorylation. To ascertain if a protein phosphatase is responsible for the activation (dephosphorylation), cells were incubated with FFA in the presence and absence of okadaic acid, an inhibitor of multiple serine/threonine protein phosphatases (28). Indeed, okadaic acid prevented dephosphorylation of FoxO3a by the toxic saturated FFA, palmitic or stearic acid (Fig. 7A). It also prevented Bim protein and mRNA induction and apoptosis by these otherwise toxic FFA (Fig. 7, A–C). Although okadaic acid can inhibit protein phosphatase type 1 (PP1) and type 2A (PP2A) activity, it is less effective *versus* PP1 (K_i of 147 nM) than PP2A (K_i of 0.032 nM). However, to exclude an effect of PP1, we

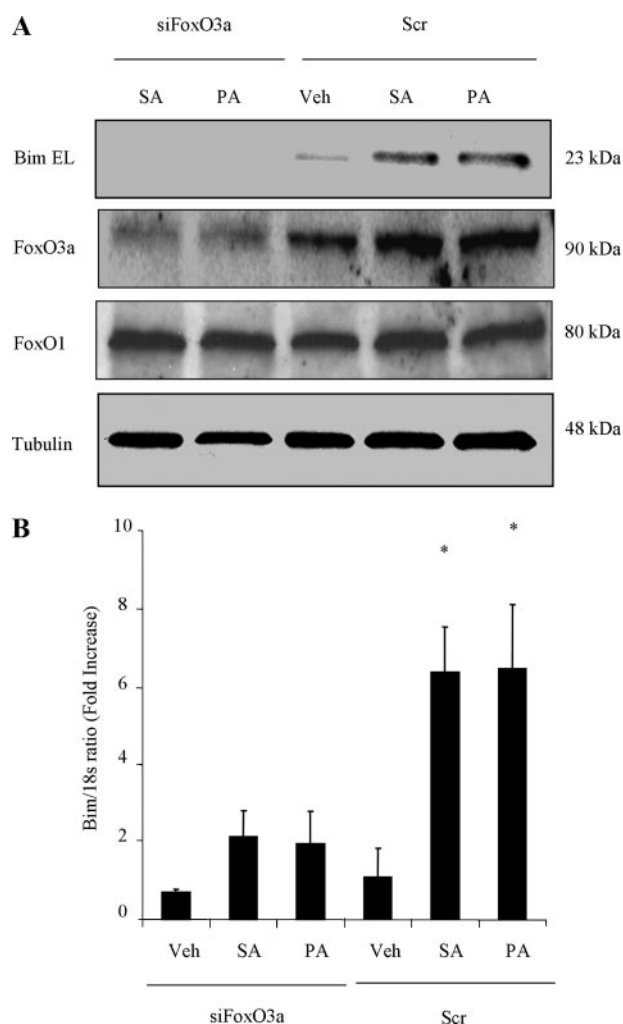


FIGURE 4. FoxO3a gene silencing decreases Bim induction by FFA. A, Huh-7 cells were transfected with a FoxO3a-specific siRNA. Forty-eight hours following transfection, cells were incubated with SA, PA (400 μ M), or vehicle for an additional 8 h. Immunoblot for Bim, FoxO3a, and FoxO1 protein expression was performed on whole cell lysates. Tubulin was used as control for protein loading. B, RNA was extracted from SA-, PA-, or vehicle-treated Huh-7 cells and quantified by real time PCR. -Fold induction was determined after normalization to 18 S. Data represent the mean and S.E. of three separate experiments. *, $p < 0.05$. Scr, scrambled.

next employed the selective PP1 inhibitor (22, 29), 1,2-dioleoyl-sn-glycero-3-phosphate, and examined its ability to reduce saturated FFA-mediated FoxO3a activation, Bim expression, and apoptosis (Fig. 8). However, this selective PP1 inhibitor neither prevented FoxO3a dephosphorylation, Bim induction, nor apoptosis as measured by the caspase-3/7 assay. These data suggest that FFA stimulate FoxO3a, activating dephosphorylation by a protein phosphatase, probably PP2A.

Saturated FFA Stimulate Protein Phosphatase 2A Activity—Because protein phosphatase 2A (PP2A) has been implicated in FoxO3a regulation (22), we next examined the role of PP2A in FFA-stimulated FoxO3a activation, Bim mRNA expression, and cell death. First, we explored if FFA affect the activity of PP2A. Indeed, PP2A activity was 3-fold greater in stearic and palmitic acid-treated cells as compared with basal values and was 2-fold greater than in oleic acid-treated cells (Fig. 9A). Not only did FFA enhance PP2A activity as assessed by a consensus

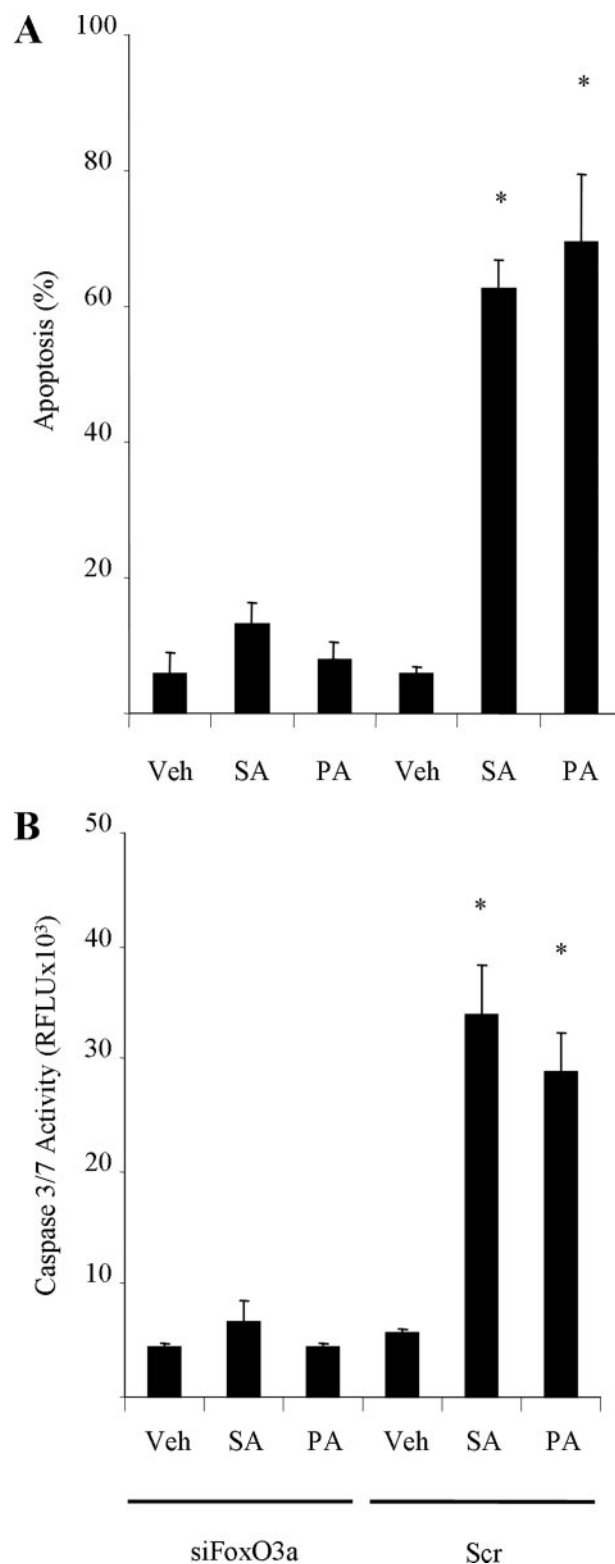


FIGURE 5. FoxO3a is a key regulator of free fatty acid-mediated apoptosis. A, Huh-7 cells were transfected with a FoxO3a siRNA. Forty-eight hours following transfection, cells were incubated with SA or PA (400 μ M) for an additional 16 h. Veh-treated cells were used as controls. Apoptosis was quantified by assessing the characteristic nuclear changes of apoptosis using the nuclear binding dye DAPI. B, in parallel studies, apoptosis was also evaluated by measuring caspase-3/7 activity. Data are mean \pm S.E. of three separate studies. *, $p < 0.05$. Scr, scrambled.

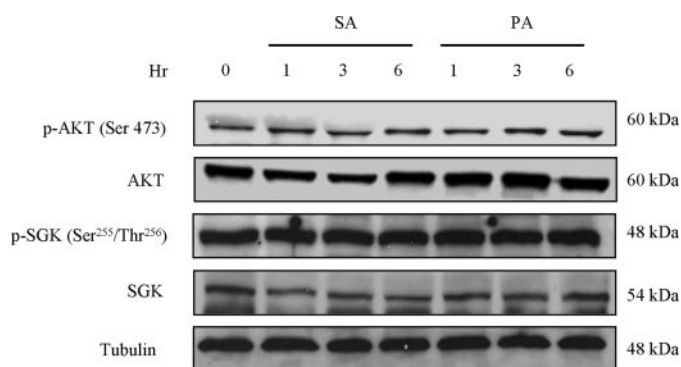


FIGURE 6. FFA treatment does not affect Akt nor SGK activation. Immunoblot analysis was performed using antibodies to total Akt and SGK and the active forms (phosphorylated) of these kinases using whole cell lysates obtained from Huh-7 cells treated with 400 μ M SA and PA at the time intervals indicated. Tubulin was used as a protein loading control. Data are mean \pm S.E. from three separate experiments. *, $p < 0.05$.

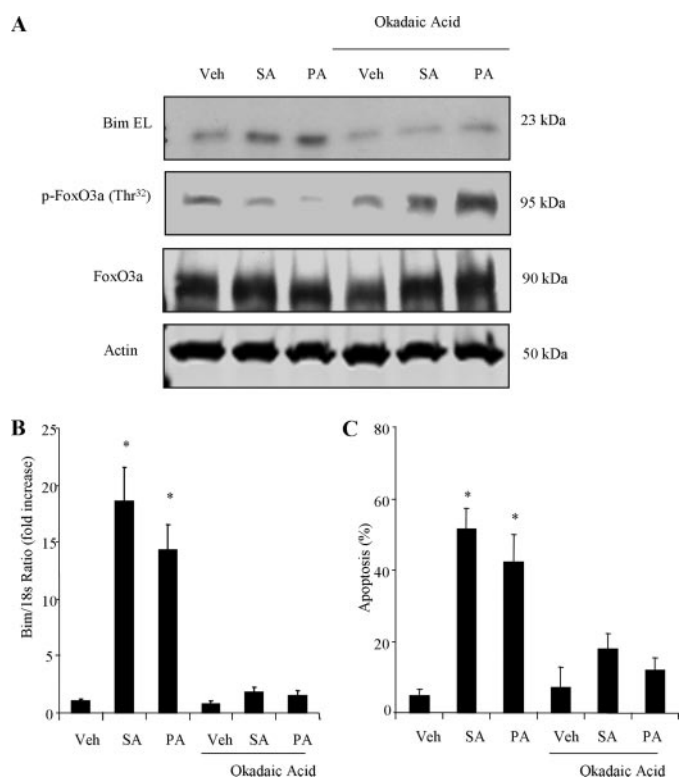


FIGURE 7. The protein phosphatase inhibitor, okadaic acid, reduces FFA-mediated dephosphorylation of FoxO3a and Bim mRNA and protein expression. A, Huh-7 cells were treated with 400 μ M SA, PA, or Veh for 6 h in the presence or absence of 100 nM okadaic acid. Whole cell lysates were subjected to immunoblot analysis for FoxO3a, phospho-FoxO3a, and Bim protein expression. Actin was used as control for protein loading. B, in parallel studies, mRNA was extracted from Huh-7 cells and Bim mRNA quantified by real time PCR. -Fold induction was determined after normalization to 18 S. C, Huh-7 cells were treated with SA and PA (400 μ M) or Veh for 16 h in the presence or absence of okadaic acid (100 nM). Cells with characteristic nuclear changes of apoptosis were quantified using the nuclear binding dye DAPI. Data represent the mean \pm S.E. of three separate studies. *, $p < 0.05$.

phosphopeptide substrate, but they also increased its activity as quantified by a FoxO3a peptide substrate containing phospho-Thr³² (Fig. 9A). In contrast, neither palmitic nor stearic acid affected PP1 phosphatase activity in this assay (data not shown). The increase in PP2A activity occurred in the absence of an increase in its cellular protein (Fig. 9B) and mRNA levels (data

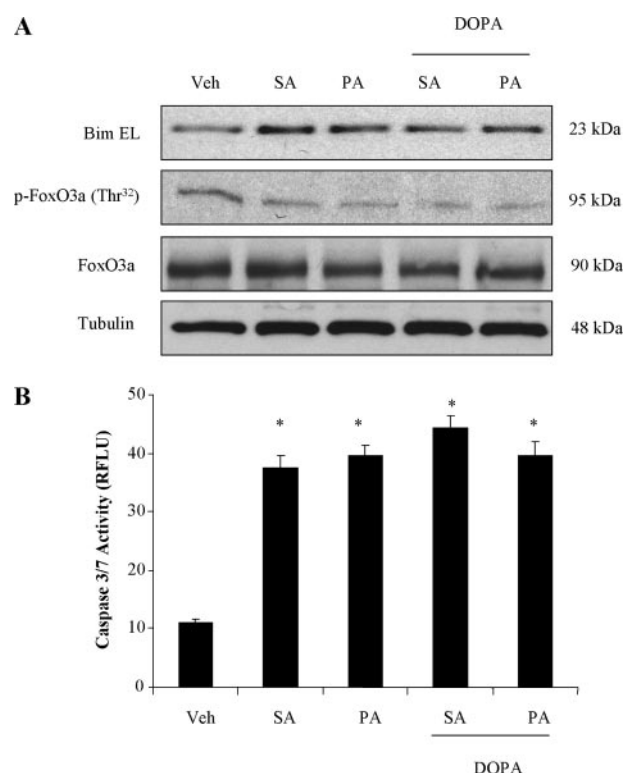


FIGURE 8. PP1 inhibition does not reduce FFA-mediated dephosphorylation of FoxO3a or Bim induction. A, Huh-7 cells were treated with 400 μ M SA, PA, or Veh for 6 h in the presence or absence of 100 nM 1,2-dioleoyl-sn-glycero-3-phosphate. Whole cell lysates were subjected to immunoblot analysis for FoxO3a, phospho-FoxO3a, and Bim protein expression. Tubulin was used as control for protein loading. B, in parallel studies, apoptosis was also evaluated by measuring caspase 3/7 activity. Huh-7 cells were treated with SA and PA (400 μ M) or Veh for 12 h in the presence or absence of 1,2-dioleoyl-sn-glycero-3-phosphate (100 nM). Data represent the mean \pm S.E. of four separate studies. *, $p < 0.05$.

not shown). Because PP2A is activated by dephosphorylation of Tyr³⁰⁷, we next examined the phosphorylation status of PP2A by phosphoimmunoblot analysis. In fact, FFA-mediated PP2A activity was associated with a reduction in Tyr³⁰⁷ phosphorylation (Fig. 9C). Next, a siRNA approach was employed to selectively knock down this protein phosphatase (Fig. 10, A–E). PP2A is composed of a family of phosphatases (30); the active enzyme consists of a heterotrimer consisting of A (scaffolding) and B (regulatory) subunits and a C (catalytic) subunit. We employed an siRNA targeting the catalytic or C α subunit for these studies. The PP2A-C α siRNA reduced the mRNA for its target, but not that for the PP1 catalytic subunit (PP1C) (Fig. 10A). It also and effectively abrogated increases in PP2A activity by FFA (Fig. 10A). Targeted siRNA knockdown of the catalytic (PP2A-C α) subunit of PP2A also reduced stearic or palmitic acid-mediated Thr³² FoxO3a dephosphorylation, Bim mRNA induction, and apoptosis (Fig. 10, B and C). Taken together, these data suggest that FFA promote FoxO3a activation by stimulating protein phosphatase 2A activity.

To elucidate the mechanism by which PP2A can regulate the activity (phosphorylation) of FoxO3a, we examined if FoxO3a is physically associated with PP2A. To confirm this postulate, we transfected Huh-7 cells with HA-FoxO3a and examined its association with PP2A by immunoprecipitation studies. Indeed, immunoprecipitation studies revealed an

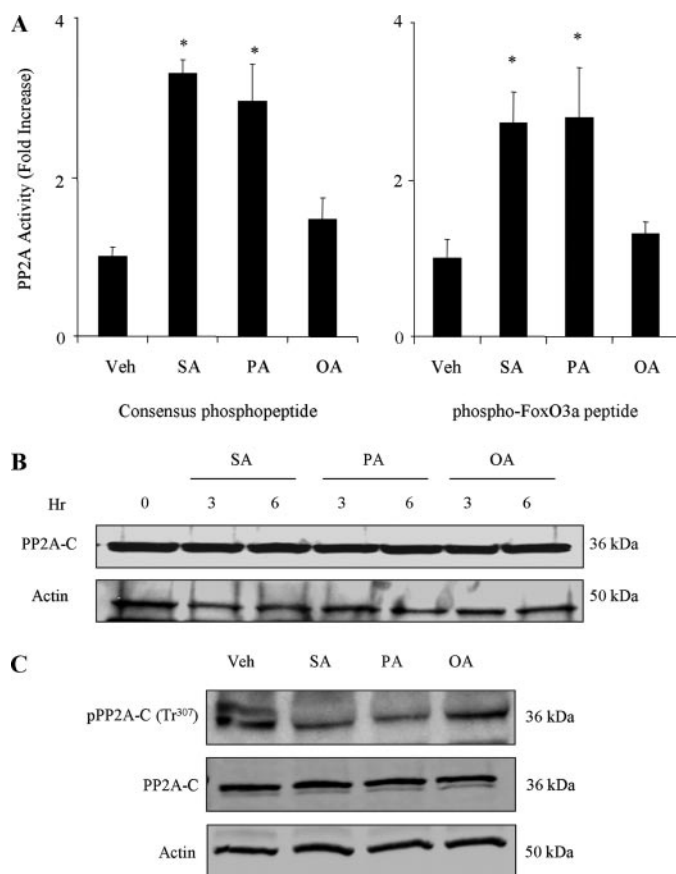


FIGURE 9. Saturated FFA activate PP2A. A, Huh-7 cells were treated with SA, PA, or OA (400 μ M) for 6 h. Veh was used as a control. PP2A-C α activity was measured in immunoprecipitates by the malachite green assay as described under "Experimental Procedures." Results are mean \pm S.E. of five separate experiments. B, Huh-7 cells were treated with SA, PA, or OA (400 μ M) for the indicated time intervals. Whole cell lysates were subjected to immunoblot analysis for PP2A-C and phospho-PP2A-C. Actin was used as a control for protein loading. C, Huh-7 cells were treated with 400 μ M SA, PA, or OA for 6 h. Veh-treated cells were used as a control. Whole cell lysates were subjected to immunoblot analysis using antibodies for total and phosphorylated (inactive form) PP2A-C. Actin was used as control for protein loading. Immunoblots are representative of three separate studies.

FFA-dependent (palmitic acid) association between FoxO3a and PP2A (Fig. 11). These observations suggest that FFA stimulate PP2A activity, which in turn dephosphorylates/activates FoxO3a.

FFA-mediated FoxO3a Dephosphorylation and Bim Expression Is Not Mediated by the *de novo* Ceramide Synthesis Pathway—Recently, it has been suggested that *de novo* ceramide synthesis may mediate the effects of saturated FFA on PP2A activity (30). To ascertain if *de novo* ceramide synthesis was responsible for FoxO3a dephosphorylation and Bim expression in our model, we employed the ceramide synthesis inhibitor fumonisins B1 (30, 31). However, this inhibitor prevented neither FoxO3a dephosphorylation nor the increase in Bim expressed following treatment of Huh-7 cells with palmitic acid (Fig. 12, A and B). It also did not prevent palmitic acid-mediated apoptosis as assessed by caspase-3/7 activity (Fig. 12C). Based on these studies, we cannot implicate *de novo* ceramide synthesis for saturated FFA-mediated FoxO3a activation, Bim induction, or apoptosis.

FFA Activates FoxO3a by Dephosphorylation in HepG2 Cells and Murine Hepatocytes—Finally, in order to establish that our observations were not unique to Huh-7 cells, we extended our study to include HepG2 cells and primary cultures of murine hepatocytes. HepG2 cells were treated with FFA (400 μ M) for 8 h, and Bim mRNA and FoxO3a activation was evaluated by immunoblot analysis. Indeed, FFA increase Bim mRNA and activate (dephosphorylate) FoxO3a (Fig. 13, A and B). Next, to investigate the role of protein phosphatases on FoxO3a activation, okadaic acid was employed. In agreement with our previous results, FFA-stimulated FoxO3a dephosphorylation was inhibited by okadaic acid in HepG2 cells (Fig. 13B). Furthermore, saturated FFA stimulate PP2A enzymatic activity (Fig. 13C), and a reduction in PP2A-C Tyr³⁰⁷ phosphorylation (Fig. 13D). FFA-mediated lipoapoptosis was also decreased by okadaic acid (Fig. 13E). FFA-induced Bim mRNA expression, dephosphorylation/activation of FoxO3a, and okadaic acid inhibition of apoptosis were also observed in primary murine hepatocytes (Fig. 14, A–C). Thus, a similar pathway of FFA-mediated FoxO3a activation was present in HepG2 and primary murine hepatocytes as observed in Huh-7 cells.

DISCUSSION

The principal findings of this study pertain to the mechanisms of FFA-mediated lipoapoptosis. The results indicate that the toxic, saturated free fatty acids, stearic and palmitic acid, but not the nontoxic monounsaturated FFA oleic acid (i) induce expression of Bim by a FoxO3a-dependent mechanism, ii) promote FoxO3a dephosphorylation (activation) by stimulating protein phosphatase 2A activity, and iii) mediate apoptosis in part by a protein phosphatase 2A/FoxO3a/Bim pathway. Modulation of this pathway is a potential therapeutic strategy for ameliorating FFA-induced hepatocyte lipoapoptosis.

In this study, we used nonesterified fatty acids or FFA at concentrations of 400 μ M incubated in the presence of albumin. The presence of albumin in our medium assures a physiologic balance between bound and free nonesterified fatty acids in the media analogous to the ratio present in plasma (32). Moreover, the fasting plasma concentrations of total FFA in human non-alcoholic steatohepatitis are in the 700 μ M range (9). Although the exact species of circulating FFA in humans with the metabolic syndrome has not been well studied, ~35% of the total serum FFA in humans are saturated (33–35). Thus, our *in vitro* cell system examining the toxicity of FFA models the circulating concentrations of these lipids in humans during metabolic disturbances.

Bim is a BH3-only protein member of the Bcl-2 family and has been implicated in mediating cell death by a wide variety of toxic stimuli, including chemotherapy, disturbances in the cellular cytoskeleton, death receptors, cytokine withdrawal, and other noxious stress stimuli (14). Although we previously implicated Bim in FFA-mediated lipoapoptosis (10), the mechanism(s) by which FFA activate Bim were not elucidated in that study. Bim is regulated by both transcriptional and post-translational mechanisms. At the post-translational level, Bim can be activated by c-Jun-N-terminal (JNK) kinase phosphorylation

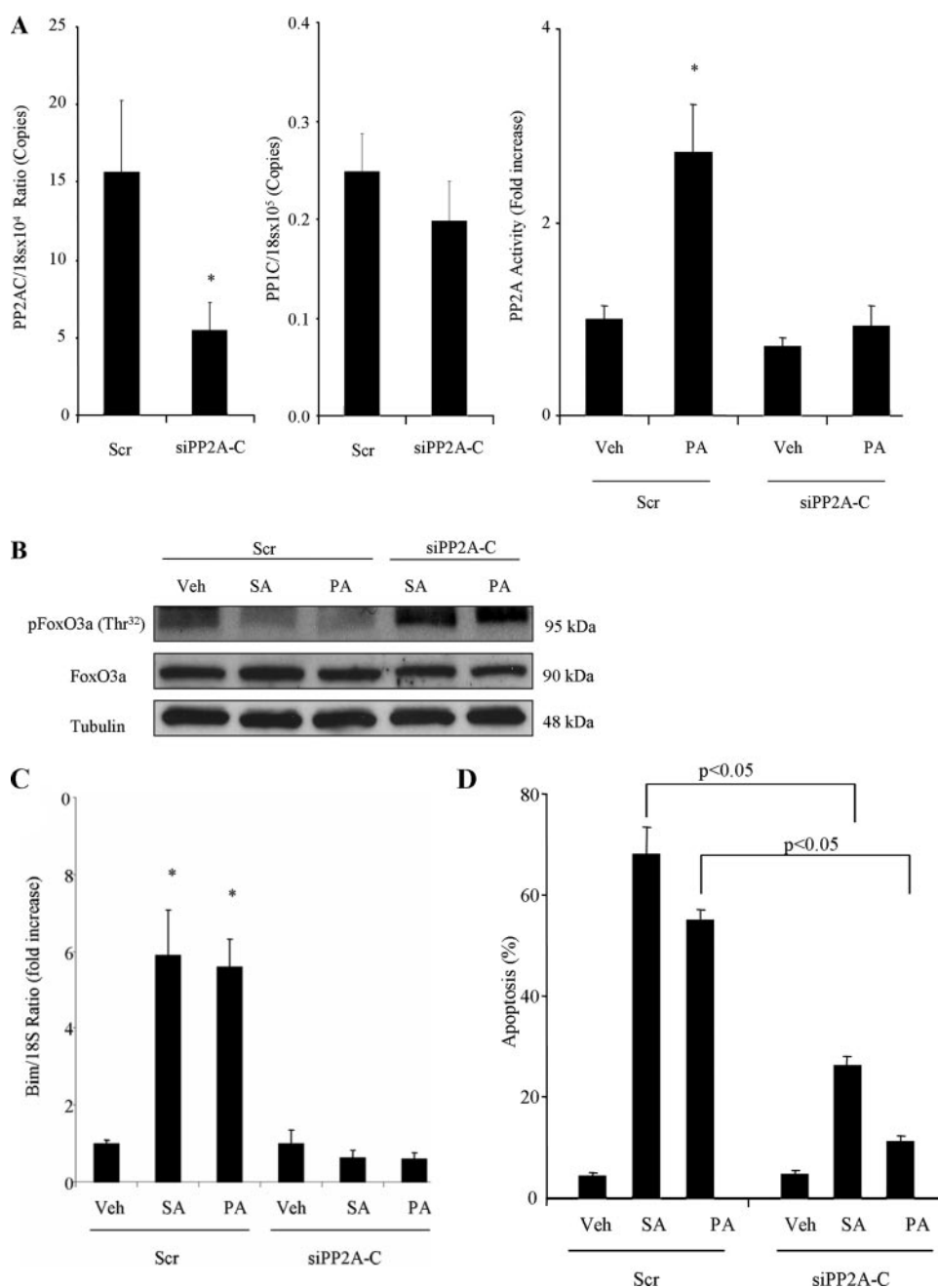


FIGURE 10. PP2A activation by saturated FFA mediates FoxO3a-dependent Bim expression. A, Huh-7 cells were transfected with an siRNA that targets PP2A-C α , and scrambled siRNA was used as transfection control. To evaluate the effectiveness of siPP2A-C α to knock down its target, real time PCR for PP2A-C α mRNA and PP1C mRNA was performed. In parallel, an assay for PP2A cellular catalytic (phosphatase) activity was performed. B, activation of FoxO3a by phosphoimmunoblot was assessed following siRNA-targeted PP2A-C α knockdown. Huh-7 cells were treated with SA or PA (400 μ M) for 6 h. C, in parallel, mRNA was extracted from SA-, PA-, or OA-treated Huh-7 cells, and Bim mRNA was quantitated by real time PCR as described under "Experimental Procedures." -Fold induction was determined after normalization to 18 S. Data represent the mean \pm S.E. of five independent experiments. D, after 48 h of transfection with PP2A-C α -targeted siRNA, Huh-7 cells were treated with saturated SA, PA, or OA (400 μ M) for 16 h. Apoptosis was assessed by quantification of the characteristic nuclear changes of apoptosis using the nuclear binding dye DAPI and a fluorescence microscope. Data are mean \pm S.E. of four independent experiments. *, $p < 0.05$. Scr, scrambled.

(36) or inhibited by extracellular receptor kinase phosphorylation, which targets the protein for proteosomal degradation (37). Bim can also be transcriptionally induced, especially by members of the FoxO family of transcription factors (18, 20, 38). The results herein suggest that toxic, saturated FFA reg-

ulate Bim by a transcriptional mechanism. Activation (dephosphorylation) of the transcription factor FoxO3a, its nuclear translocation, and binding to the Bim promoter were all observed following treatment of Huh-7 cells with FFA. Furthermore, siRNA-targeted knockdown of FoxO3a abrogated the increase in Bim and cell death by the saturated FFA, stearic and palmitic acid. Taken together, these data indicate that FFA regulate Bim predominantly via a transcriptional mechanism, although the possibility of concomitant post-translational activation by JNK cannot be excluded, especially given the known activation of JNK by FFA (10).

Enhanced activity of FoxO3a has been implicated in the expression of additional apoptosis effectors, in addition to Bim. For example, FoxO3a can induce the expression of the BH3-only protein Puma (p53-up-regulated modulator of apoptosis) (39), and the death ligands Fas-L (23) and Trail (40). However, in our prior studies, siRNA-targeted knockdown of Bim was sufficient to attenuate FFA-induced hepatocyte apoptosis, whereas inhibition of the death receptor pathway by enforced expression of dominant negative FADD did not prevent cell death (10). Therefore, at least *in vitro*, expression of these other apoptosis effectors does not appear to contribute to hepatocyte cell death by FFA.

FoxO transcription factors are generally regulated at the post-transcriptional level by phosphorylation and acetylation (41). In regard to FoxO3a, there are three conserved phosphorylation sites, T1 (Thr³²), S1 (Ser²⁵³), and S2 (Ser³¹⁵), that are recognized by Akt and SGK with different affinities (23, 24). However, it is unlikely that a reduction in kinase activity resulted in FoxO3a dephosphorylation and activation.

We failed to observe a reduction in the phosphorylated or active form of Akt and SGK in FFA-treated cells (Fig. 6). Therefore, we focused on FoxO3a dephosphorylation by PP2A. Our observations demonstrate stimulation of PP2A activity following treatment of cells by FFA; conversely,

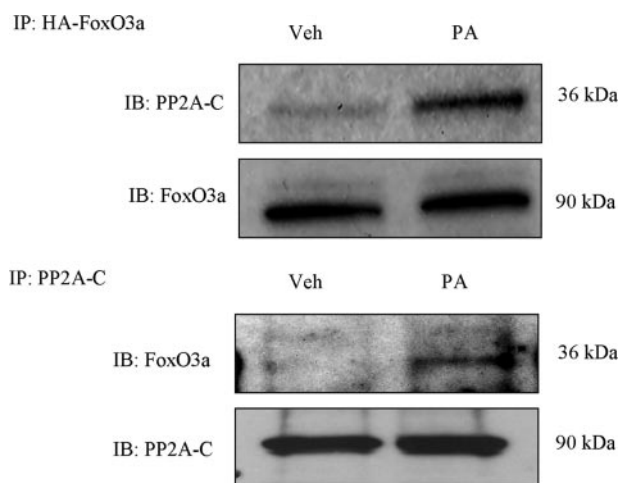


FIGURE 11. PP2A interacts with FoxO3a following cellular treatment with palmitic acid. Huh-7 cells stably transfected with HA-FoxO3a were treated with PA (400 μ M) for 6 h. Veh was used as a control. HA-FoxO3a was immunoprecipitated (IP) from whole cell lysates, and immunocomplexes were subjected to immunoblot (IB) analysis with antibodies to FoxO3a and PP2A-C. In parallel studies, Huh-7 cells were treated with PA (400 μ M) or vehicle for 6 h. PP2A-C was immunoprecipitated from whole cell lysates, and immunocomplexes were subjected to immunoblot analysis with antibodies for FoxO3a and PP2A-C.

siRNA-targeted knockdown or pharmacologic inhibition of PP2A blocked FoxO3a activation. These data suggest that FFA may stimulate PP2A. This observation has significant implications for liver pathophysiology in NASH given the large number of proteins affected by protein phosphatase activity.

It is beyond the scope of the current study to ascertain how FFA effect changes in PP2A activity. However, considerable information is available to help guide such investigations. PP2A is a heterotrimer complex composed of a catalytic subunit (PP2A-C), which is associated with a scaffolding A subunit (PP2A-A) and a regulatory subunit (PP2A-B). Only two isoforms of the A (α A and α B) and C (α C and β C) subunits have been identified (42), although there are four families of B subunits and each subfamily has multiple isoforms (42). The B subunit provides stability to the heterotrimer, influencing substrate specificity and subcellular localization. Protein phosphatase 2A can be regulated by phosphorylation of the catalytic subunit. The catalytic subunit of PP2A can be phosphorylated by the tyrosine kinases pp60^{v-src} and pp56^{lck}, the epidermal growth factor, and insulin receptors (43, 44). The phosphorylation occurs on Tyr³⁰⁷, which is located in the C terminus of PP2A-C, and results in inactivation of the enzyme. Tyrosine phosphorylation of PP2A-C is enhanced in the presence of the phosphatase inhibitor okadaic acid, suggesting that, under different conditions, PP2A-C can rapidly reactivate itself in an autodephosphorylation response. Indeed, our results demonstrate that PP2A-C decreases its phosphorylation at Tyr³⁰⁷ under FFA treatment, and thereby increases its catalytic activity.

Protein phosphatase 2A is expressed in all cell types and is involved in a wide range of cellular processes, including cell cycle regulation, cell morphology, development, signal transduction, translation, and apoptosis. Recent studies have suggested that PP2A has a critical role in the regulation of

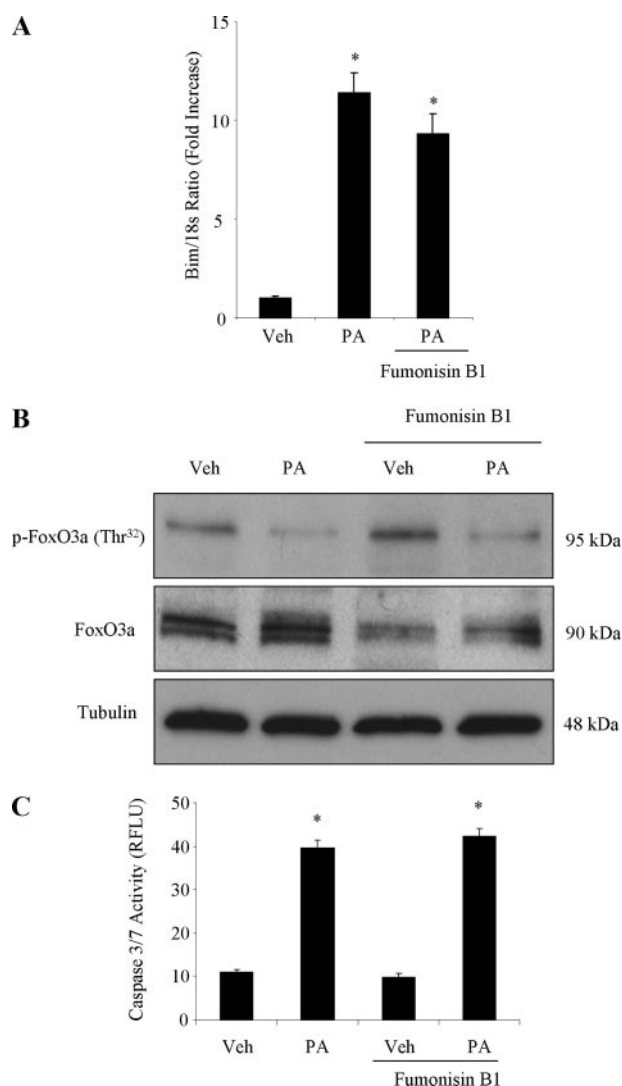


FIGURE 12. FFA-mediated FoxO3a dephosphorylation and Bim expression is not mediated by the *de novo* ceramide synthesis pathway. A, Huh-7 cells were treated with 400 μ M PA or Veh for 6 h in the presence or absence of 15 μ M fumonisin B1, an inhibitor of *de novo* formation of ceramide. mRNA was extracted, and Bim mRNA was quantified by real time PCR. -Fold induction was determined after normalization to 18 S. Data represent the mean \pm S.E. of four independent studies. *, $p < 0.05$. B, in parallel studies, whole cell lysates were subjected to immunoblot analysis for FoxO3a and phospho-FoxO3a. Tubulin was used as control for protein loading. C, apoptosis was also evaluated by measuring caspase-3/7 activity. Huh-7 cells were treated with PA (400 μ M) or Veh for 12 h in the presence or absence of fumonisin B1 (15 μ M). Data represent the mean \pm S.E. of four separate studies. *, $p < 0.05$.

apoptosis (22, 45–51). The activity of PP2A can regulate the responsiveness to death receptor-mediated cell death by Fas (45), tumor necrosis factor- α (46), and TRAIL (47) via regulation of mitogen-activated protein kinases, such as p38, extracellular signal-regulated kinase, and JNK. Furthermore, PP2A has been implicated in regulation of the intrinsic pathway of cell death by dephosphorylation and inhibition of Bcl-2 (49) or by dephosphorylation and activation of Bad (50) and Bax (51). PP2A has also been proposed to induce Bim expression by modulating Akt activation (22); however, in our current studies, neither Akt nor SGK was affected by FFA treatment. Our studies extend these observations by

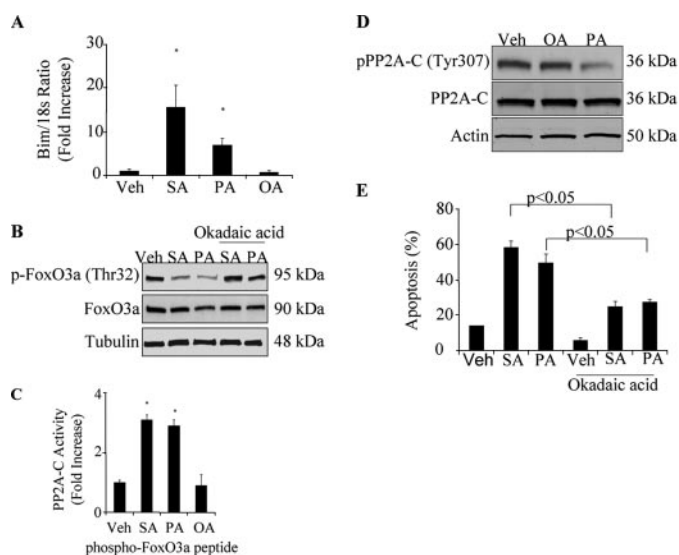


FIGURE 13. FFA activate FoxO3a by dephosphorylation and increase PP2A activity in HepG2 cells. A, HepG2 cells were treated with SA, PA, or OA (400 μ M) for 8 h. mRNA was extracted, and real time PCR was performed for Bim mRNA. Data are mean \pm S.E. of five separate experiments. *, $p < 0.05$. B, HepG2 cells were incubated with SA or PA (400 μ M) or vehicle in the presence or absence of okadaic acid (100 nM) for 8 h. The phosphorylation status of FoxO3a was examined by phosphoimmunoblot analysis. Tubulin was used as control for protein loading. C, HepG2 cells were treated with SA, PA, or OA (400 μ M) for 8 h. Vehicle was used as a control. PP2A-C activity was assayed in immune complexes following its immunoprecipitation using a phospho-FoxO3a peptide. Results are the mean \pm S.E. of four separate experiments. D, HepG2 cells were incubated for 6 h with OA or PA (400 μ M) or Veh as a control. The phosphorylation status of PP2A-C at Tyr³⁰⁷ was examined by phosphoimmunoblot analysis. E, HepG2 cells were treated with SA or PA (400 μ M) for 16 h in the presence or absence of okadaic acid (100 nM). Apoptosis were assessed by quantification of the characteristic nuclear changes of apoptosis using the nuclear binding dye DAPI. Data are mean \pm S.E. of three separate experiments. *, $p < 0.05$.

suggesting that PP2A also drives dephosphorylation (activation) of FoxO3a, thereby promoting apoptosis.

One of the findings of our study is that saturated FFA were more cytotoxic than monounsaturated FFA. These data are in accord with our prior observation (10) and a wide variety of different cell types, including pancreatic β -cell (31, 52), astrocytes (53), neurons (54), granulose (55) and Leydig cells (56), breast cancer cells (57), endothelial cells (58, 59), and cardiac myocytes (60). The mechanism by which FFA are more toxic than unsaturated FFA have not been identified. Recently, saturated FFA, but not unsaturated FFA, have been proposed as ligands of the Toll-like receptor 4 (61, 62). Perhaps, like insulin resistance, FFA-mediated cytotoxicity requires engagement of this membrane receptor.

Our cellular model provides additional insight into the potential mechanisms by which FFA induce hepatocyte lipapoptosis. Apoptosis is regulated by members of the Bcl-2 family of proteins. Antiapoptotic, multidomain members of this family (*i.e.* Bcl-2, Bcl-X_L, Mcl-1 (myeloid cell leukemia 1), and Bcl-w) prevent apoptosis and function as cell guardians. In contrast, proapoptotic members of this family (*i.e.* Bak (Bcl-2 antagonist/killer) and Bax) serve as executioners in the apoptotic program. BH3-only proteins, such as Bim, are the biosensors of cellular stress and engage the apoptosis program by either depressing antiapoptotic or directly ligating and activating proapoptotic multidomain Bcl-2 proteins

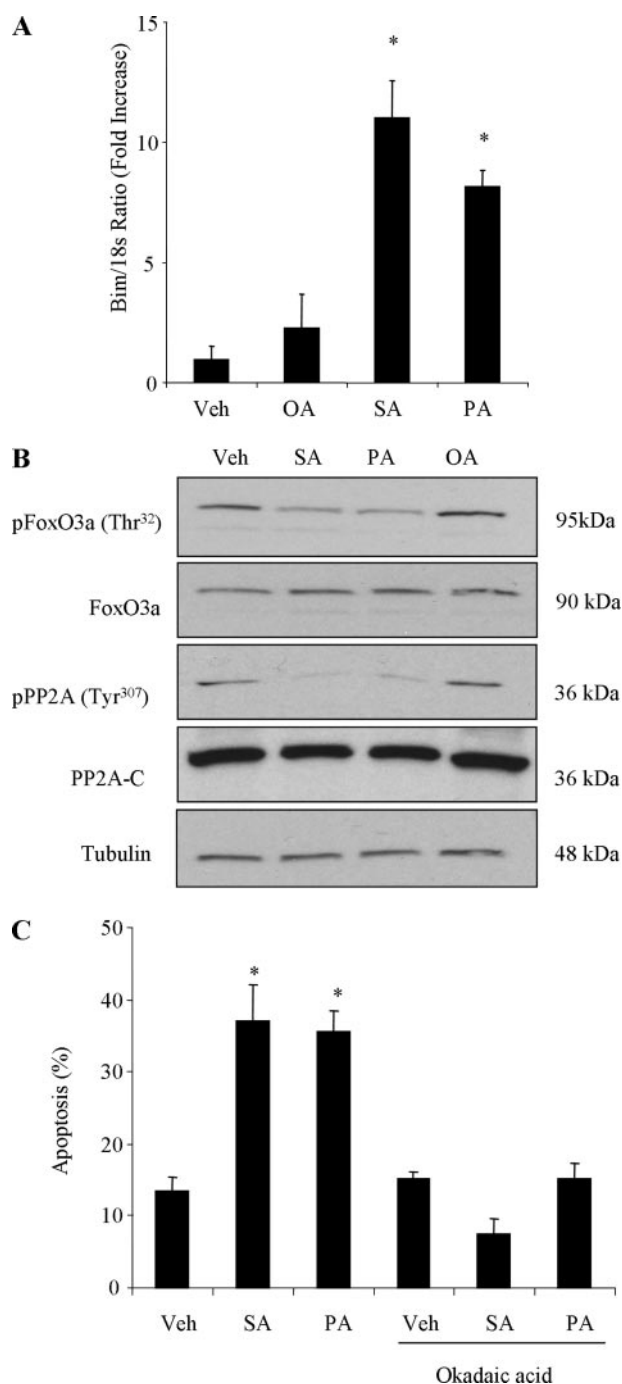


FIGURE 14. FFA activate FoxO3a and increase PP2A activity in primary murine hepatocytes. A, primary murine hepatocytes were treated with SA, PA, or OA (400 μ M) or vehicle for 6 h. Next, mRNA was extracted, and Bim mRNA was quantified by real time PCR. Data are mean \pm S.E. of six separate experiments. B, primary murine hepatocytes were treated with SA, PA, or OA (400 μ M) for 8 h. Veh was used as a control. The phosphorylation status of FoxO3a (Thr³²) and PP2A-C (Tyr³⁰⁷) was examined by immunoblot analysis. Tubulin was used as control for protein loading. C, primary cultured cells were treated with SA or PA (400 μ M) for 8 h in the presence or absence of okadaic acid (30 nM). Apoptosis was assessed by quantification of the characteristic nuclear morphology of apoptosis using the nuclear binding dye DAPI. Data are mean \pm S.E. of four individual experiments. *, $p < 0.05$.

(14). Our previously published data suggested that both JNK and Bim were necessary for Bax activation and cell death by toxic FFA (10). Perhaps JNK through a kinase cascade promotes Bax dissociation from cytosolic binding partners

and/or its translocation to mitochondria (63). Once Bax has translocated to mitochondria, Bim may in turn directly bind and activate Bax or indirectly activate this proapoptotic protein by derepressing antiapoptotic Bcl-2 proteins (64). Once fully activated, Bax induces mitochondrial dysfunction, release of cytochrome *c*, activation of effector caspases, and cell death (65). Thus, FFA stimulation of JNK plus FoxoO3a activity appears to work in concert to induce cell death.

Hepatocyte lipoapoptosis is a cardinal feature of NASH, a growing public health problem (3, 12). Our current data provide insight into the mechanisms of FFA-induced lipoapoptosis, namely stimulation of FoxO3a-dependent Bim expression. Modulation of this pathway is a potential therapeutic strategy to ameliorate NASH.

REFERENCES

- Neuschwander-Tetri, B. A., and Caldwell, S. H. (2003) *Hepatology* **37**, 1202–1219
- Matteoni, C. A., Younossi, Z. M., Gramlich, T., Boparai, N., Liu, Y. C., and McCullough, A. J. (1999) *Gastroenterology* **116**, 1413–1419
- Angulo, P., Keach, J. C., Batts, K. P., and Lindor, K. D. (1999) *Hepatology* **30**, 1356–1362
- Pagano, G., Pacini, G., Musso, G., Gambino, R., Mecca, F., Depetris, N., Cassader, M., David, E., Cavallo-Perin, P., and Rizzetto, M. (2002) *Hepatology* **35**, 367–372
- Bugianesi, E., McCullough, A. J., and Marchesini, G. (2005) *Hepatology* **42**, 987–1000
- Donnelly, K. L., Smith, C. I., Schwarzenberg, S. J., Jessurun, J., Boldt, M. D., and Parks, E. J. (2005) *J. Clin. Invest.* **115**, 1343–1351
- Nehra, V., Angulo, P., Buchman, A. L., and Lindor, K. D. (2001) *Dig. Dis. Sci.* **46**, 2347–2352
- Feldstein, A. E., Canbay, A., Guicciardi, M. E., Higuchi, H., Bronk, S. F., and Gores, G. J. (2003) *J. Hepatol.* **39**, 978–983
- Belfort, R., Harrison, S. A., Brown, K., Darland, C., Finch, J., Hardies, J., Balas, B., Gastaldelli, A., Tio, F., Pulcini, J., Berria, R., Ma, J. Z., Dwivedi, S., Havranek, R., Fincke, C., DeFronzo, R., Bannayan, G. A., Schenker, S., and Cusi, K. (2006) *N. Engl. J. Med.* **355**, 2297–2307
- Malhi, H., Bronk, S. F., Werneburg, N. W., and Gores, G. J. (2006) *J. Biol. Chem.* **281**, 12093–12101
- Unger, R. H. (2002) *Annu. Rev. Med.* **53**, 319–336
- Feldstein, A. E., Canbay, A., Angulo, P., Taniai, M., Burgart, L. J., Lindor, K. D., and Gores, G. J. (2003) *Gastroenterology* **125**, 437–443
- Wieckowska, A., Zein, N. N., Yerian, L. M., Lopez, A. R., McCullough, A. J., and Feldstein, A. E. (2006) *Hepatology* **44**, 27–33
- Willis, S. N., and Adams, J. M. (2005) *Curr. Opin. Cell Biol.* **17**, 617–625
- Martinou, J. C., and Green, D. R. (2001) *Nat. Rev. Mol. Cell Biol.* **2**, 63–67
- Guicciardi, M. E., and Gores, G. J. (2005) *Gut* **54**, 1024–1033
- Bouillet, P., Huang, D. C., O'Reilly, L. A., Puthalakath, H., O'Connor, L., Cory, S., Adams, J. M., and Strasser, A. (2000) *Ann. N. Y. Acad. Sci.* **926**, 83–89
- Dijkers, P. F., Medema, R. H., Lammers, J. W., Koenderman, L., and Coffey, P. J. (2000) *Curr. Biol.* **10**, 1201–1204
- Stahl, M., Dijkers, P. F., Kops, G. J., Lens, S. M., Coffey, P. J., Burgering, B. M., and Medema, R. H. (2002) *J. Immunol.* **168**, 5024–5031
- Gilley, J., Coffey, P. J., and Ham, J. (2003) *J. Cell Biol.* **162**, 613–622
- Van Der Heide, L. P., Hoekman, M. F., and Smidt, M. P. (2004) *Biochem. J.* **380**, 297–309
- Yin, K. J., Hsu, C. Y., Hu, X. Y., Chen, H., Chen, S. W., Xu, J., and Lee, J. M. (2006) *J. Neurosci.* **26**, 2290–2299
- Brunet, A., Bonni, A., Zigmond, M. J., Lin, M. Z., Juo, P., Hu, L. S., Anderson, M. J., Arden, K. C., Blenis, J., and Greenberg, M. E. (1999) *Cell* **96**, 857–868
- Brunet, A., Park, J., Tran, H., Hu, L. S., Hemmings, B. A., and Greenberg, M. E. (2001) *Mol. Cell Biol.* **21**, 952–965
- Faubion, W. A., Guicciardi, M. E., Miyoshi, H., Bronk, S. F., Roberts, P. J., Svingen, P. A., Kaufmann, S. H., and Gores, G. J. (1999) *J. Clin. Invest.* **103**, 137–145
- Hu, M. C., Lee, D. F., Xia, W., Golfman, L. S., Ou-Yang, F., Yang, J. Y., Zou, Y., Bao, S., Hanada, N., Saso, H., Kobayashi, R., and Hung, M. C. (2004) *Cell* **117**, 225–237
- Tang, E. D., Nunez, G., Barr, F. G., and Guan, K. L. (1999) *J. Biol. Chem.* **274**, 16741–16746
- Sontag, E. (2001) *Cell. Signal.* **13**, 7–16
- Gallego, M., and Virshup, D. M. (2005) *Curr. Opin. Cell Biol.* **17**, 197–202
- Wu, Y., Song, P., Xu, J., Zhang, M., and Zou, M. H. (2007) *J. Biol. Chem.* **282**, 9777–9788
- Shimabukuro, M., Zhou, Y. T., Levi, M., and Unger, R. H. (1998) *Proc. Natl. Acad. Sci. U. S. A.* **95**, 2498–2502
- Richieri, G. V., and Kleinfeld, A. M. (1995) *J. Lipid Res.* **36**, 229–240
- Fernandez-Real, J. M., Broch, M., Vendrell, J., and Ricart, W. (2003) *Diabetes Care* **26**, 1362–1368
- Leskinen, M. H., Solakivi, T., Kunnas, T., Alho, H., and Nikkari, S. T. (2005) *Scand. J. Clin. Lab. Invest.* **65**, 485–490
- Summers, L. K., Fielding, B. A., Bradshaw, H. A., Ilic, V., Beysen, C., Clark, M. L., Moore, N. R., and Frayn, K. N. (2002) *Diabetologia* **45**, 369–377
- Putch, G. V., Le, S., Frank, S., Besirli, C. G., Clark, K., Chu, B., Alix, S., Youle, R. J., LaMarche, A., Maroney, A. C., and Johnson, E. M., Jr. (2003) *Neuron* **38**, 899–914
- Ley, R., Balmanno, K., Hadfield, K., Weston, C., and Cook, S. J. (2003) *J. Biol. Chem.* **278**, 18811–18816
- Sunters, A., Fernandez de Mattos, S., Stahl, M., Brosens, J. J., Zoumpoulidou, G., Saunders, C. A., Coffey, P. J., Medema, R. H., Coombes, R. C., and Lam, E. W. (2003) *J. Biol. Chem.* **278**, 49795–49805
- You, H., Pellegrini, M., Tsuchihara, K., Yamamoto, K., Hacker, G., Erlacher, M., Villunger, A., and Mak, T. W. (2006) *J. Exp. Med.* **203**, 1657–1663
- Modur, V., Nagarajan, R., Evers, B. M., and Milbrandt, J. (2002) *J. Biol. Chem.* **277**, 47928–47937
- Accili, D., and Arden, K. C. (2004) *Cell* **117**, 421–426
- Kowluru, A. (2005) *Biochem. Pharmacol.* **69**, 1681–1691
- Chen, J., Martin, B. L., and Brautigan, D. L. (1992) *Science* **257**, 1261–1264
- Chen, J., Parsons, S., and Brautigan, D. L. (1994) *J. Biol. Chem.* **269**, 7957–7962
- Alvarado-Kristensson, M., and Andersson, T. (2005) *J. Biol. Chem.* **280**, 6238–6244
- Ray, R. M., Bhattacharya, S., and Johnson, L. R. (2005) *J. Biol. Chem.* **280**, 31091–31100
- Harmala-Brasken, A. S., Mikhailov, A., Soderstrom, T. S., Meinander, A., Holmstrom, T. H., Damuni, Z., and Eriksson, J. E. (2003) *Oncogene* **22**, 7677–7686
- Chatfield, K., and Eastman, A. (2004) *Biochem. Biophys. Res. Commun.* **323**, 1313–1320
- Deng, X., Ito, T., Carr, B., Mumby, M., and May, W. S., Jr. (1998) *J. Biol. Chem.* **273**, 34157–34163
- Chiang, C. W., Harris, G., Ellig, C., Masters, S. C., Subramanian, R., Shenolikar, S., Wadzinski, B. E., and Yang, E. (2001) *Blood* **97**, 1289–1297
- Xin, M., and Deng, X. (2006) *J. Biol. Chem.* **281**, 18859–18867
- Karaskov, E., Scott, C., Zhang, L., Teodoro, T., Ravazzola, M., and Volchuk, A. (2006) *Endocrinology* **147**, 3398–3407
- Patil, S., and Chan, C. (2005) *Neurosci. Lett.* **384**, 288–293
- Ulloa, J. E., Casiano, C. A., and De Leon, M. (2003) *J. Neurochem.* **84**, 655–668
- Mu, Y. M., Yanase, T., Nishi, Y., Tanaka, A., Saito, M., Jin, C. H., Mukasa, C., Okabe, T., Nomura, M., Goto, K., and Nawata, H. (2001) *Endocrinology* **142**, 3590–3597
- Lu, Z. H., Mu, Y. M., Wang, B. A., Li, X. L., Lu, J. M., Li, J. Y., Pan, C. Y., Yanase, T., and Nawata, H. (2003) *Biochem. Biophys. Res. Commun.* **303**, 1002–1007
- Hardy, S., El-Asaad, W., Przybytkowski, E., Joly, E., Prentki, M., and Langelier, Y. (2003) *J. Biol. Chem.* **278**, 31861–31870
- Artwohl, M., Roden, M., Waldhausl, W., Freudenthaler, A., and Baumgartner-Parzer, S. M. (2004) *FASEB J.* **18**, 146–148
- Yamagishi, S., Okamoto, T., Amano, S., Inagaki, Y., Koga, K., Koga, M.,

- Choei, H., Sasaki, N., Kikuchi, S., Takeuchi, M., and Makita, Z. (2002) *Mol. Med.* **8**, 179–184
60. Hickson-Bick, D. L., Sparagna, G. C., Buja, L. M., and McMillin, J. B. (2002) *Am. J. Physiol. Heart Circ. Physiol.* **282**, H656–H664
61. Lee, J. Y., Sohn, K. H., Rhee, S. H., and Hwang, D. (2001) *J. Biol. Chem.* **276**, 16683–16689
62. Shi, H., Kokoeva, M. V., Inouye, K., Tzameli, I., Yin, H., and Flier, J. S. (2006) *J. Clin. Invest.* **116**, 3015–3025
63. Tsuruta, F., Sunayama, J., Mori, Y., Hattori, S., Shimizu, S., Tsujimoto, Y., Yoshioka, K., Masuyama, N., and Gotoh, Y. (2004) *EMBO J.* **23**, 1889–1899
64. Baskin-Bey, E. S., and Gores, G. J. (2005) *Am. J. Physiol.* **289**, G987–G990
65. Wei, M. C., Zong, W. X., Cheng, E. H., Lindsten, T., Panoutsakopoulou, V., Ross, A. J., Roth, K. A., MacGregor, G. R., Thompson, C. B., and Korsmeyer, S. J. (2001) *Science* **292**, 727–730

Transcriptional Regulation of Bim by FoxO3A Mediates Hepatocyte Lipoapoptosis

Fernando J. Barreyro, Shogo Kobayashi, Steven F. Bronk, Nathan W. Werneburg,
Harmeet Malhi and Gregory J. Gores

J. Biol. Chem. 2007, 282:27141-27154.

doi: 10.1074/jbc.M704391200 originally published online July 11, 2007

Access the most updated version of this article at doi: [10.1074/jbc.M704391200](https://doi.org/10.1074/jbc.M704391200)

Alerts:

- [When this article is cited](#)
- [When a correction for this article is posted](#)

[Click here](#) to choose from all of JBC's e-mail alerts

This article cites 65 references, 26 of which can be accessed free at
<http://www.jbc.org/content/282/37/27141.full.html#ref-list-1>